Eur Biophys J (1987) 15: 47–58

European Biophysics Journal

A new approach to polarized fluorescence using phase and modulation fluorometry

II. Experiments with 1,6-diphenyl-1,3,5-hexatriene in lipid bilayers

H. Pottel[1], B. W. Van der Meer[2]*, W. Herreman[1], and H. Depauw[3]

[1] Interdisciplinair Research Centrum, Katholieke Universiteit Leuven, Campus Kortrijk, B-8500 Kortrijk, Belgium
[2] Department of Pharmacology, University of Texas, Health Science Center at Dallas, 5323 Harry Hines Boulevard, Dallas, Texas 75235, USA
[3] RUCA-Laboratorium voor Biochemie van de mens, Rijksuniversitair Centrum Antwerpen, 171 Groenenborgerlaan, B-2020 Antwerpen, Belgium

Received April 1, 1986/Accepted in revised form January 3, 1987

Abstract. In the preceding paper, an alternative method is described for obtaining information about the reorientational behavior of a fluorophore in a membrane system from frequency domain measurements. To demonstrate this new analysis procedure, we present data for the probe-molecule 1,6-diphenyl-1,3,5-hexatriene (DPH) in L-α-dimyristoyl- and L-α-dipalmitoylphosphatidylcholine (DMPC and DPPC) obtained with two different phase fluorometers: the SLM 4800A Subnanosecond Spectrofluorometer which has only three fixed frequencies available (6, 18 and 30 MHz) and the recently constructed continuously variable multifrequency phasefluorometer (Gratton and Limkeman 1983).

It will be shown that reasonable information about the anisotropy behavior of a fluorophore can be obtained even if only three frequencies are used. The phase modulation technique was also used to check the new expression for the anisotropy, $r(t)$, called the general model and introduced by Van der Meer et al. (1984). The parameters $\langle P_2 \rangle$, $\langle P_4 \rangle$ and D, obtained from the nonlinear least squares fit (Bevington 1969) for this general model, confirm the results from the pulse technique of Ameloot and coworkers (Ameloot et al. 1984; Pottel et al. 1986).

Key words: Fluorescence anisotropy, phase fluorometry, diphenylhexatriene

Introduction

Differential polarized phase modulation fluorometry has been used widely to investigate the behavior of fluorescent probe-molecules such as DPH (Lakowicz and Prendergast 1978a, b; Lakowicz et al. 1979, 1985; Zavoico et al. 1985), fluorescein (Lakowicz et al. 1985), perylene (Lakowicz et al. 1985; Chong et al. 1985; Mantulin and Weber 1977) and other fluorophores (Zavoico et al. 1985; Mantulin and Weber 1977; Lakowicz et al. 1984a) in isotropic solvents and anisotropic lipid bilayers. The motions of these probes are dependent upon the fluorophore itself and its surrounding environment.

In the technique of differential polarized phase fluorometry, one measures the difference in phase between the parallel and perpendicular components of the fluorescence emission, when the sample is excited by vertically polarized (parallel), sinusoidally modulated light.

The theoretical basis of this technique has been developed by Weber (1977) and it was also Weber who extended the theory to fluorophores in a hindered environment (Weber 1978). This theory describes the depolarizing rotations of the fluorophore by its apparent rotational rate (R) and the limiting fluorescence anisotropy (r_∞) at times long compared with the fluorescence lifetime.

Through the combined use of both steady-state anisotropy measurements and differential phase measurements, Lakowicz et al. (1978a, b, 1979) have demonstrated that one may obtain unique solutions for both R and r_∞. At that time, fluorescence lifetimes and the tangent of the differential phase ($\tan \Delta$) were measured by the phase shift method (Spencer and Weber 1969, 1970) using only one, two or three light modulations frequencies.

With the construction of a continuously variable frequency cross-correlation phase-fluorometer (Gratton and Limkeman 1983), it became possible to determine the time-dependent anisotropy decay $r(t)$ from frequency domain measurements. Lakowicz et al. (1985) used the newly developed phase fluorometer, which operates at modulation frequencies from 1 to 200 MHz, to demonstrate the applicability

* Present address: OMRF, Thrombosis/Hematology Research Program, 825 N.E. 13th Street, Oklahoma City, OK 73104, USA

of the instrument to systems exhibiting several decays of anisotropy. They measured the phase angle difference ($\Delta = \Phi_\perp - \Phi_\parallel$) between the parallel and perpendicular components of the fluorescence emission and the ratio of the modulated fluorescence intensities ($m_\parallel/m_\perp$). With a nonlinear least squares method (Bevington 1969; Lakowicz et al. 1984b), they resolved single, double and triple exponential decays of anisotropy and the hindered rotational motions of fluorophores within lipid bilayers.

It is our intention to demonstrate here the applicability of the Sine-Cosine Transform method, described in the previous paper (Van der Meer et al. 1987), by presenting results for the anisotropy decay parameters for DPH in DMPC and DPPC for two different models of anisotropy decays. These results fully confirm those obtained by Ameloot et al. (1984) using the pulse technique.

Theoretical background

In the previous paper, the theoretical background of a phase-modulation experiment is given. It is shown that to determine the time-dependent anisotropy $r(t)$ – whether the differential or transform method is used – analytical expressions for $r(t)$ and the total fluorescence intensity decay $I(t)$ in terms of a set of unknown parameters are needed. Moreover, the unknown anisotropy decay parameters can only be obtained if the lifetime(s) of the excited state of the fluorophore is (are) determined. Therefore, an analytical expression for $I(t)$ has to be assumed.

The lifetime(s) of the fluorophore can be obtained from the sine and cosine transform (denoted by S_T and G_T resp.) of the total fluorescence intensity, using a non-linear least squares method (Bevington 1969; Lakowicz et al. 1984b) which minimizes the χ^2 value, defined as:

$$\chi^2 = \sum_\omega \frac{1}{\sigma^2}(S_{T_c} - S_{T_m})^2 + \sum_\omega \frac{1}{\sigma^2}(G_{T_c} - G_{T_m})^2 \qquad (1)$$

where

$$S_{T_c} = \int_0^\infty I(t) \sin\omega t \, dt \Big/ \int_0^\infty I(t)\, dt \qquad (2a)$$

$$G_{T_c} = \int_0^\infty I(t) \cos\omega t \, dt \Big/ \int_0^\infty I(t)\, dt \qquad (2b)$$

are the calculated values; S_{T_m} and G_{T_m} are the measured values obtained from the measured phase, Φ_T, and modulation, m_T (differential method):

$$S_T = m_T \sin\Phi_T \qquad (3a)$$

$$G_T = m_T \cos\Phi_T \qquad (3b)$$

or from the measured phases $\Phi_\parallel$, $\Phi_\perp$, and the modulations $m_\parallel$, $m_\perp$ and steady-state anisotropy, r_s (transform method):

$$S_T = \tfrac{1}{3}(1+2r_s)\, m_\parallel \sin\Phi_\parallel + \tfrac{2}{3}(1-r_s)\, m_\perp \sin\Phi_\perp \qquad (4a)$$

$$G_T = \tfrac{1}{3}(1+2r_s)\, m_\parallel \cos\Phi_\parallel + \tfrac{2}{3}(1-r_s)\, m_\perp \cos\Phi_\perp \qquad (4b)$$

σ is the estimated standard deviation of the measured S_T and G_T and is here fixed to $\sigma = 0.005$, corresponding to a value of $\Delta m = 0.003$, $\Delta\Phi = 0.3°$ (and $\Delta r_s = 0.001$).

Once the lifetime(s) of the fluorophore is (are) known, the anisotropy decay parameters can be determined, following the transform method, from the constructed "Sine and Cosine transforms" S_D^* and G_D^* and the steady-state anisotropy:

$$S_D^* = \int_0^\infty I(t)\, r(t) \sin\omega t \, dt \Big/ \int_0^\infty I(t)\, dt$$
$$= \tfrac{1}{3}(1+2r_s)\, m_\parallel \sin\Phi_\parallel - \tfrac{1}{3}(1-r_s)\, m_\perp \sin\Phi_\perp \qquad (5a)$$

$$G_D^* = \int_0^\infty I(t)\, r(t) \cos\omega t \, dt \Big/ \int_0^\infty I(t)\, dt$$
$$= \tfrac{1}{3}(1+2r_s)\, m_\parallel \cos\Phi_\parallel - \tfrac{1}{3}(1-r_s)\, m_\perp \cos\Phi_\perp \qquad (5b)$$

$$r_s = \int_0^\infty I(t)\, r(t)\, dt \Big/ \int_0^\infty I(t)\, dt\,. \qquad (5c)$$

The non-linear least squares method minimizes the χ^2-value, here defined as:

$$\chi^2 = \sum_\omega \frac{1}{\sigma_1^2}(S_{D_c}^* - S_{D_m}^*)^2 + \sum_\omega \frac{1}{\sigma_1^2}(G_{D_c}^* - G_{D_m}^*)^2 + \frac{1}{\sigma_2^2}(r_{s_c} - r_{s_m})^2, \qquad (6)$$

where $S_{D_c}^*$, $G_{D_c}^*$ and r_{s_c} are calculated from Eqs. (5a–c), assuming analytical expressions for $I(t)$ and $r(t)$, and $S_{D_m}^*$ and $G_{D_m}^*$ are the measured values calculated from Eqs. (5a–b) using the experimentally obtained phases $\Phi_\parallel$, $\Phi_\perp$, modulations $m_\parallel$, $m_\perp$ and steady-state anisotropy, r_s. The standard deviations σ_1 and σ_2 are fixed at 0.002 and 0.001, corresponding to estimated errors in the modulation $\Delta m = 0.003$ and phase $\Delta\Phi = 0.2°$ (Lakowicz et al. 1985).

Note that if the modulation is turned off ($\omega = 0$), it follows from Eq. (5b) that $G_D^* = r_s$ or one can consider the steady-state anisotropy as the cosine transform value at zero modulation frequency.

Materials and methods

1. Measurements performed on the SLM 4800A subnanosecond spectrofluorometer on small unilamellar vesicles

Materials. Diphenylhexatriene (DPH) was obtained from Aldrich. Dipalmitoylphosphatidylcholine

(DPPC) and dimyristoylphosphatidylcholine (DMPC) came from Sigma Chemicals.

Unilamellar lipid vesicles were prepared essentially as described by Johnson and Zilversmit (1975). Stock solutions of DPPC and DMPC were prepared in chloroform/methanol (2/1). The required amount of lipid was dried from the stock solution under a stream of N_2. The dried lipid was resuspended in diethylether and redried under N_2 to form a thin film in a test tube. Sufficient buffer (10 m*M Tris*, pH 7.4) was added to give a lipid suspension of 0.5 m*M*. This suspension was agitated for 10 min under N_2 with a Vortex mixer and then allowed to stand for 1 h at room temperature. The lipid suspension was then sonicated with a Braun-Sonic 300 Homogenisator (Quigly-Rochester, Inc.) using a 4.0 mm diameter Titanium probe until a clear dispersion was obtained. The sonicated solution was centrifuged for 16 min at 37,000 g to remove large liposomes. Liposomes were kept at 4 °C under N_2 and used within 48 h after preparation.

Diphenylhexatriene was made up in tetrahydrofuran at a concentration of 1 m*M*. For labelling, this solution was diluted 1000-fold by adding to a vigourously stirred buffer solution (10 m*M Tris*, pH 7.4). DPH was then added to the lipid vesicles at a ratio of 1 molecule DPH for every 500 phospholipid molecules. Vesicles and probe were incubated for 1.5 h at 37 °C.

Methods. Static and dynamic fluorescence parameters were recorded on a SLM 4800A Subnanosecond Spectrofluorometer equipped with a Hewlett-Packard 85 calculator and a 7225A plotter. Temperature was controlled by a Lauda thermostated water bath and measured inside the fluorescent cuvettes with an AD590 probe (Analog Devices). Glan-Thompson polarizers were used in the excitation and emission sides. Dynamic measurements were performed by the cross-correlation phase method described by Spencer and Weber (1969). The excitation beam was modulated by a Debye-Sears modulator at a frequency of either 6, 18 or 30 MHz. Phase shift and modulation of the fluorescence emission of the sample were measured relative to a glycogen-scattering solution. The excitation polarizer was in the vertical position and the emission polarizer was set at 0°, 90° or 54.7°. In all these measurements the following instrumental conditions were utilized: excitation wavelength 360 nm, emission filters Schott KV 399.

Experiments with DPH in DMPC and DPPC vesicles were performed at various temperatures. At each temperature the phases and modulations Φ_T and m_T (emission polarizer set at 54.7°), $\Phi_\parallel$ and $m_\parallel$ (emission polarizer at 0°), $\Phi_\perp$ and $m_\perp$ (emission polarizer at 90°) were measured at the three available frequencies. The steady-state anisotropy r_s was measured in the same instrument with the modulation turned off.

The phase difference and demodulation was read again for both the scatterer and sample. Therefore, the phase shift due to fluorescence is (Spencer and Weber 1969)

$$\Phi = \Phi_{\text{fluorescence}} - \Phi_{\text{scatterer}} \tag{7a}$$

and the modulation

$$m = m_{\text{fluorescence}}/m_{\text{scatterer}} \,. \tag{7b}$$

2. Measurements on the continuously variable frequency phase fluorometer of Gratton and Limkeman (1983) on small unilamellar vesicles

Materials. Unilamellar lipid vesicles were prepared as follows: The required amount of DMPC or DPPC was dissolved in chloroform and DPH was added to assure a probe/lipid ratio of 1 : 500. Lipids and DPH were co-dried under a stream of nitrogen and subsequently under vacuum for several hours. Sufficient buffer (10 m*M* Hepes, pH 7.0, 0.1 m*M* KCl, degassed before use) was added to give a lipid suspension of 0.3 m*M*. The lipids were allowed to hydrate for 0.5 h at 37 °C under nitrogen and the suspension was then vortexed to disperse the lipids. The lipid suspension was sonicated for 2 h above the phase transition temperature in a bath sonicator device. The sonicated solution was centrifuged for 1 h at 50,000 g and the supernatant was taken for measurements. Vesicles were used within 10 h after preparation.

Methods. Experiments with DPH in DMPC and DPPC vesicles at various temperatures above and below the phase transition of the lipid system were performed. Each experiment consisted of the measurement of $\Phi_\parallel$, $\Phi_\perp$, $m_\parallel$ and $m_\perp$ at 7 or 8 modulation frequencies (2, 4, 8, 16, 32, 50, 70 and 100 MHz). The steady-state anisotropy, r_s, was measured in the same instrument by turning off the modulation. The instrument used was the variable multifrequency phase modulation fluorometer constructed by Gratton and Limkeman (1983). The apparatus uses cross-correlation detection. The excitation source was an Argon ion laser (Spectra Physics, Inc., model 164) which was tuned for output at 351 nm. More specific information about this instrument can be found in the paper of Gratton and Limkeman (1983).

For both instruments the lifetime of the fluorophore was obtained from the differential and/or the transform method following the procedure described in the previous section. For two different anisotropy decay functions [$r(t)$ = monoexponential + constant and $r(t)$ = general model (Van der Meer 1984)] the

unknown parameters (respectively r_∞, R and $\langle P_2 \rangle$, $\langle P_4 \rangle$, D) in the constructed sine and cosine transforms (Eqs. (5a – b)) and the steady-state anisotropy (Eq. (5c)) were obtained from the already mentioned non-linear least squares method which minimizes the χ^2 value defined in Eq. (6). The uncertainties in the parameters were estimated from the diagonal elements of the error matrix (Bevington 1969). The initial anisotropy r_0 was always held fixed at 0.380 as determined by Ameloot et al. (1984).

Results and discussion

DPH lifetimes can be obtained as explained in the section "theoretical background" from the differential method and the transform method. The measurements we performed on the commercially available instrument (SLM instrument, Urbana, IL) developed by Spencer and Weber (1969, 1970), at three modulation frequencies 6, 18 and 30 MHz, made it possible to compare the results obtained from both methods. The conclusion from our data – whether these data were obtained with the transform or differential method – is that the total fluorescence intensity of DPH is reasonably well described by a single exponential function. This conclusion, however, is a controversial one. A double exponential decay of DPH in both pure gel and pure liquid crystalline phase of DMPC and DPPC bilayers was found by several workers using the pulse technique (Ameloot et al. 1984; Chen et al. 1977; Dale et al. 1977; Stubbs et al. 1981). In contrast, by phase fluorometry, a mono-exponential decay has been found for many phospholipid bilayers above the phase-transition temperature (Lentz et al. 1976; Barrow and Lentz 1985; Klausner et al. 1980) and also above and below the phase transition (Lakowicz et al. 1985; Depauw et al. 1985). It is not the purpose of this paper to discuss this perhaps controversial conclusion. However, it is clear that if a double exponential decay is considered, the expressions for sine and cosine transforms S_D^* and G_D^*, presented in the appendix, have to be modified (see for instance the appendix in the preceding paper).

Consider the normalized mono-exponential decay function for the total fluorescence intensity:

$$I(t) = \frac{1}{\tau} \exp(-t/\tau) . \tag{8}$$

Using Eq. (8), the sine and cosine transforms as defined in Eqs. (2a – b) can be expressed as:

$$S_{T_c} = \frac{\omega\tau}{(1+\omega^2\tau^2)} \tag{9a}$$

$$G_{T_c} = \frac{1}{(1+\omega^2\tau^2)} . \tag{9b}$$

Table 1. Comparison of the single lifetime τ for DPH in DMPC and DPPC vesicles obtained with the transform and differential method

Lipid	Temperature [°C]	Transform method		Differential method	
		τ [ns]	χ_r^2	τ [ns]	χ_r^2
DMPC	14.2	10.6 (0.2) [a]	5.52	10.9 (0.2)	4.05
DMPC	24.2	9.8 (0.2)	4.80	10.1 (0.1)	2.53
DMPC	34.1	8.8 (0.1)	3.85	8.9 (0.2)	9.38
DPPC	45.5	8.48 (0.09)	2.61	8.7 (0.1)	3.54
DPPC	55.6	7.6 (0.1)	6.14	7.7 (0.1)	4.94

[a] Standard errors between parentheses

In Table 1 the results are given for the single lifetime τ obtained from the non-linear least squares method minimizing χ^2 defined in Eq. (1). In this equation S_{T_c} and G_{T_c} given in Eqs. (9a – b) are introduced. S_{T_m} and G_{T_m} are calculated from the measured phase Φ_T and modulation m_T (differential method) using Eqs. (3a – b) and also from the phases $\Phi_\parallel$, $\Phi_\perp$, modulations $m_\parallel$, $m_\perp$ and the steady-state anisotropy, r_s (transform method) using Eqs. (4a – b). The χ_r^2 is a measure for the goodness of fit and is here defined as:

$$\chi_r^2 = \frac{\chi^2}{(2NF-1)} , \tag{10}$$

where NF is the number of frequencies used.

As can be seen from Table 1 the lifetime obtained from both methods is essentially the same. In Fig. 1 the sine and cosine transforms S_T and G_T as calculated from Eqs. (9a – b), with the obtained lifetime $\tau = 8.7$ ns, are plotted for DPH in DPPC at a temperature of 45.5°. The lifetime measurements on the instrument of Gratton and Limkeman (1983) were performed using the transform method. In Fig. 2 an example for DPH in DPPC at $T = 38.6°$ is shown.

Once the lifetime is determined, the anisotropy decay parameters can be obtained by fitting Eqs. (5a – c) to the experimental data, using the non-linear least squares procedure which minimizes the χ^2-value as defined in Eq. (6), if an analytical expression for $r(t)$ is assumed.

We performed experiments with DPH embedded in two lipid systems, DMPC and DPPC, at various temperatures. From the same experimental phases $\Phi_\parallel$ and $\Phi_\perp$, modulations $m_\parallel$ and $m_\perp$ and the steady-state fluorescence anisotropy r_s, we calculated, by

Table 2. Anisotropy decay parameters for DPH in DPPC and DMPC vesicles obtained with the transform method

Membranes	T [°C]	τ [ns]	r_s	$6R$ [ns^{-1}]	r_∞	χ_r^2	$\langle P_2 \rangle$	$\langle P_4 \rangle$	D [ns^{-1}]	χ_r^2
DMPC	13.0	10.2 (0.1)	0.320	0.26 (0.06)	0.299 (0.006)	2.45	0.873 (0.028)	0.781 (0.034)	0.016 (0.007)	3.54
DMPC	14.2′	10.9 (0.2)	0.3368	0.69 (0.46)	0.331 (0.004)	3.12	0.934 (0.015)	0.812 (0.062)	0.015 (0.010)	4.10
DMPC	24.2′	10.1 (0.1)	0.2200	0.63 (0.14)	0.194 (0.007)	6.20	0.711 (0.019)	0.771 (0.056)	0.46 (0.21)	8.90
DMPC	34.1′	8.8 (0.1)	0.0967	0.80 (0.07)	0.057 (0.004)	2.21	0.375 (0.024)	0.447 (0.059)	0.26 (0.06)	2.52
DMPC	34.2	8.65 (0.05)	0.090	0.81 (0.04)	0.050 (0.002)	1.58	0.338 (0.010)	0.552 (0.009)	0.50 (0.02)	1.01
DPPC	25.6	9.39 (0.09)	0.345	0.80 (0.21)	0.339 (0.002)	0.84	0.943 (0.003)	0.821 (0.023)	0.013 (0.003)	0.92
DPPC	38.6	9.60 (0.06)	0.215	2.67 (0.36)	0.208 (0.001)	0.66	0.739 (0.002)	0.622 (0.016)	0.41 (0.02)	0.58
DPPC	45.5′	8.48 (0.09)	0.0934	1.41 (0.13)	0.070 (0.003)	1.06	0.423 (0.007)	0.493 (0.028)	0.52 (0.05)	0.80
DPPC	47.8	7.70 (0.04)	0.080	1.43 (0.10)	0.054 (0.002)	2.27	0.362 (0.006)	0.459 (0.013)	0.49 (0.02)	0.84
DPPC	55.6′	7.7 (0.1)	0.0625	1.55 (0.16)	0.036 (0.003)	1.52	0.301 (0.012)	0.413 (0.023)	0.53 (0.06)	1.80

The data marked with ′ are obtained with the SLM 4800A Subnanosecond Spectrofluorometer which has only three fixed frequencies 6, 18 and 30 MHz. The other data are obtained with the continuously variable phase-fluorometer constructed by Gratton and Limkeman at 7 or 8 modulation frequencies: 2, 4, 8, 16, 32, 50, 70 and 100 MHz. In parentheses the estimated deviations as obtained from the diagonal elements of the error matrix (Bevington 1969) are given

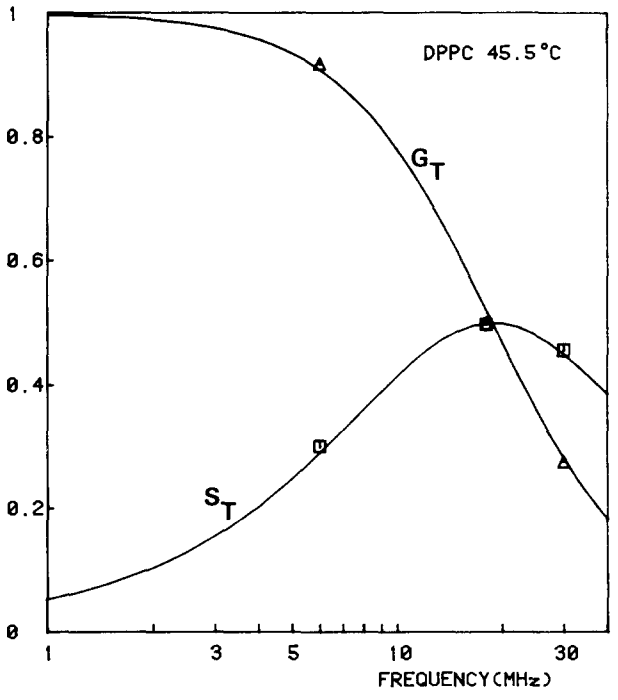

Fig. 1. Sine and cosine transforms S_T and G_T as a function of frequency obtained from the differential method. The experimental phases Φ_T and modulations m_T obtained from the differential method for DPH in DPPC at 45.5 °C were used to calculate the values for $S_T = m_T \sin \Phi_T$ (□) and $G_T = m_T \cos \Phi_T$ (△). The best fit using a mono-exponential fluorescence decay for S_T and G_T is also shown (*solid lines*). ($\tau = 8.7$ ns, $\chi_r^2 = 3.54$)

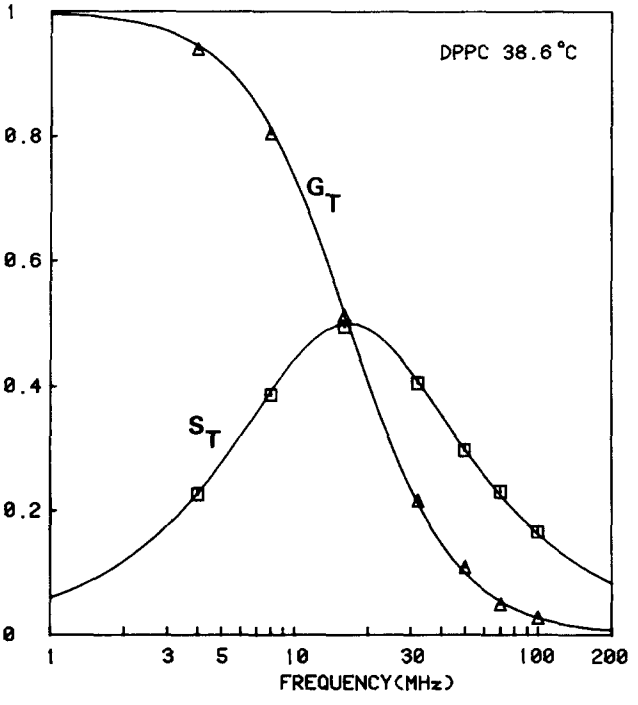

Fig. 2. Sine and cosine transforms S_T and G_T as a function of frequency. The experimental phases Φ_T and modulations m_T obtained from the transform method for DPH in DPPC at 38.6 °C were used to calculate the values for $S_T = m_T \sin \Phi_T$ (□) and $G_T = m_T \cos \Phi_T$ (△). The best fit using a mono-exponential fluorescence decay for S_T and G_T is also shown (*solid lines*). ($\tau = 9.60$ ns, $\chi_r^2 = 1.13$)

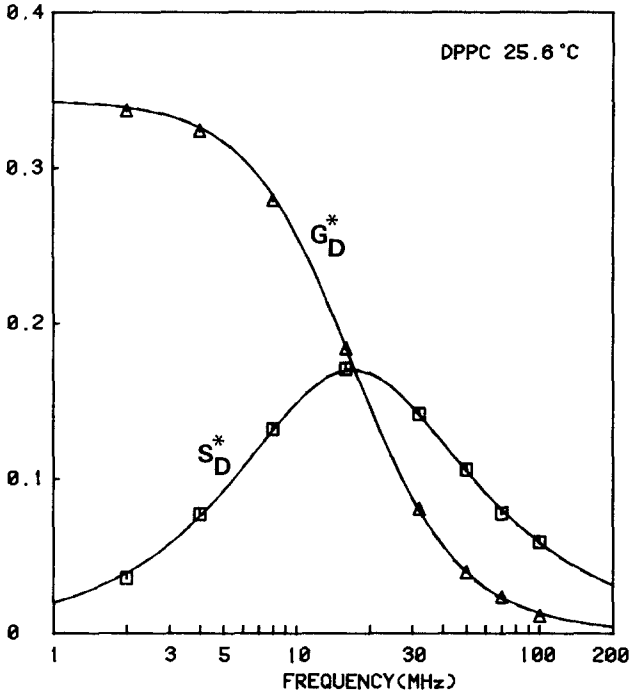

Fig. 3.

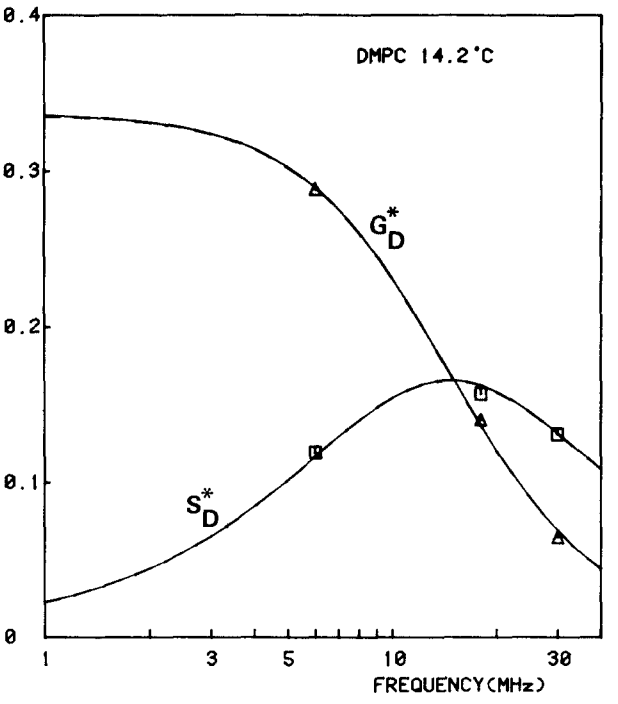

Fig. 5.

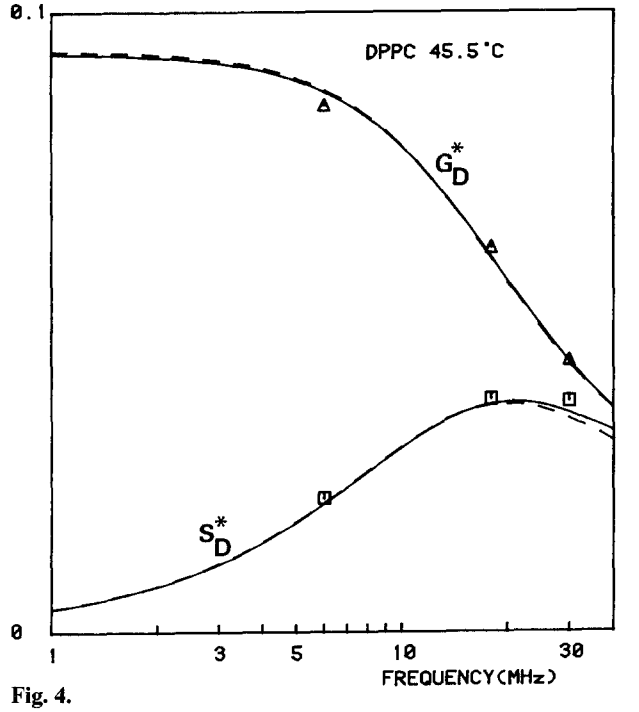

Fig. 4.

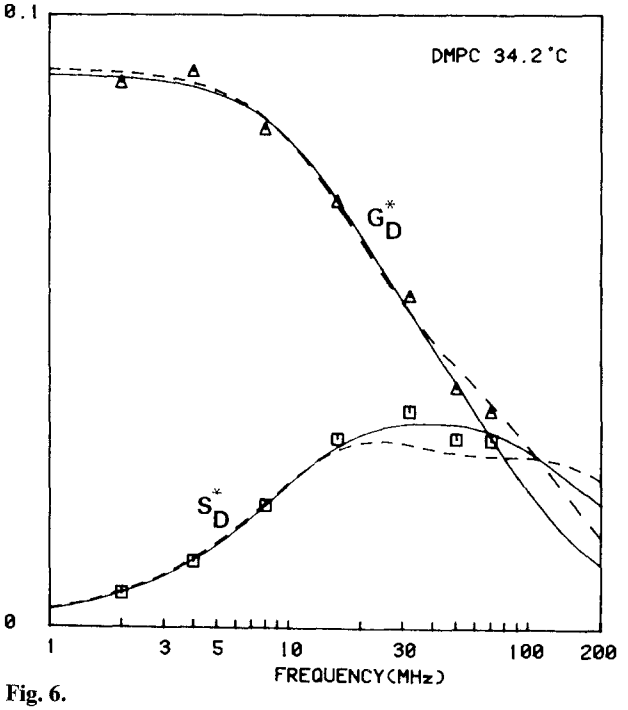

Fig. 6.

Figs. 3–6. Sine and cosine transforms S_D^* and G_D^* as a function of frequency. The experimental phases $\Phi_\parallel$, $\Phi_\perp$, modulations $m_\parallel$, $m_\perp$ and the steady-state anisotropy r_s obtained following the transform method, for DPH in DMPC and DPPC, above and below the phase transitions of the lipid systems, were used to calculate the values for S_D^* and G_D^*. Fits for S_D^* and G_D^* using the single exponential fluorescence decay and the hindered rotator model (Eq. (11)) (*dashed curves*) or the general model (Eq. (12)) (*solid curves*) are shown

the use of a non-linear least squares procedure, the parameters for two different analytical expressions for the fluorescence anisotropy, $r(t)$. The results are given in Table 2. These two different expressions for $r(t)$ are the hindered rotator model (Weber 1978) and the general model (Van der Meer et al. 1984).

$$(1)\quad r(t) = (r_0 - r_\infty)\exp(-Rt) + r_\infty\,, \tag{11}$$

where r_0 is the initial anisotropy, held fixed in the analysis to a value of 0.380, r_∞ is the limiting anisotropy and R^{-1} is a rotational relaxation time (ns).

$$(2)\quad r(t) = r_0\left[\langle P_2\rangle^2 + \beta_0\exp(-\alpha_0 t) + 2\beta_1\exp(-\alpha_1 t) + 2\beta_2\exp(-\alpha_2 t)\right], \tag{12}$$

where β_i and α_i are functions of the second and fourth rank orientational order parameters $\langle P_2\rangle$ and $\langle P_4\rangle$ and the rotational diffusion constant D $(=D_\perp)$. The explicit expressions for β_i and α_i are given in the appendix. This analytical expression for $r(t)$ is based on a new approximate solution of the rotational diffusion equation and is treated at length in the papers of Van der Meer et al. (1984) and Ameloot et al. (1984), where it is called the general model. Similar results for β_i and α_i have also been derived by Szabo (1984). The analytical expressions for the sine and cosine transforms S_D^* and G_D^*, calculated from Eqs. (5a–b) using Eq. (8) for $I(t)$ and Eqs. (11) and (12) for $r(t)$ are also given in the appendix.

In the paper of Ameloot et al. (1984) it was shown that the general model (Eq. (12)) always described the time-dependent anisotropy $r(t)$ of DPH in DMPC and DPPC better than the mono-exponential expression in Eq. (11). The discrepancy was most pronounced above the phase transition temperature of the vesicle system ($T_{t_r}=24.3°$ for DMPC and $T_{t_r}=41°$ for DPPC). As can be seen from the χ_r^2-values in Table 2, the general model indeed describes the behavior of DPH above the phase transition better than the mono-exponential model.

Below the phase transition, the differences in χ_r^2 between the two possible expressions for $r(t)$ are rather small but in favour of the mono-exponential decay indicating that the motion of DPH below T_{t_r} is far less complex than above T_{t_r}. These results confirm the results of Ameloot et al. (1984) where the pulsed method has been used.

In Figs. 3 and 4 the constructed sine an cosine transforms S_D^* and G_D^* for DPH in DPPC at 25.6° and at 45.5° are shown. The dashed curves represent the calculated S_D^* and G_D^* using the parameters R and r_∞ from Table 2. The solid curves are the calculated S_D^* and G_D^* obtained from the general model parameters in Table 2. Analogous drawings for DPH in DMPC at 14.2° and 34.2° are shown in Figs. 5 and 6. Below the phase transition, there was no visible difference between the two anisotropy decay expressions used, as can be seen from Figs. 3 and 5. The discrepancy between the two possible anisotropy decays is most pronounced above the phase transition as indicated by the χ_r^2-values in Table 2 (see Figs.4 and 6).

The ($\langle P_2\rangle$, $\langle P_4\rangle$) data from Table 2 has been shown in the ($\langle P_2\rangle$, $\langle P_4\rangle$)-plane (Fig. 7) together with three ($\langle P_2\rangle$, $\langle P_4\rangle$) relations, calculated from three different one-parameter distribution functions using

$$\langle P_2\rangle = \int_0^\pi P_2(\cos\theta)\, f(\theta)\sin\theta\,\mathrm{d}\theta \tag{13a}$$

$$\langle P_4\rangle = \int_0^\pi P_4(\cos\theta)\, f(\theta)\sin\theta\,\mathrm{d}\theta\,, \tag{13b}$$

where for curve (1), $f(\theta)$ is the cone-distribution (Kinosita et al. 1977), for curve (2), $f(\theta)$ is the Gaussian distribution (Maier-Saupe model) and curve (3) is calculated from the $\langle P_4\rangle$-distribution (Pottel et al. 1986; Zannoni 1979).

From Table 2 and Fig. 7 it can be seen that the general model yields high $\langle P_4\rangle$-values. A possible distribution function for DPH in DMPC and DPPC has recently been proposed by Pottel et al. (1986). The distribution function has the form

$$f(\theta) = Z^{-1}\int_0^\pi \exp\left[\lambda_4 P_4(\cos\theta)\right]\sin\theta\,\mathrm{d}\theta\,, \tag{14}$$

where Z is a normalization constant. This distribution is based on the "$l=4$ potential" (Zannoni 1979) and is therefore called "the $\langle P_4\rangle$-distribution". Because λ_4 is the only parameter in this distribution function, $\langle P_2\rangle$ and $\langle P_4\rangle$, as calculated from Eqs. (13) and (14), are related to each other. This relation is represented by curve (3) in the ($\langle P_2\rangle$, $\langle P_4\rangle$)-plane and is a characteristic property of the $\langle P_4\rangle$-distribution (Fig. 7).

We have reanalyzed the data obtained with the general model analysis, assuming a priori the relation between $\langle P_2\rangle$ and $\langle P_4\rangle$ which can be calculated numerically from Eq. (14) and Eqs. (13a–b). An approximation of the numerical relation for $\langle P_2\rangle > 0.250$ is given by

$$\begin{aligned}\langle P_4\rangle = {} & 0.824 - 4.288\langle P_2\rangle + 11.628\langle P_2\rangle^2 \\ & + 10.367\langle P_2\rangle^3 - 69.304\langle P_2\rangle^4 + 52.955\langle P_2\rangle^5 \\ & + 79.577\langle P_2\rangle^6 - 134.051\langle P_2\rangle^7 \\ & + 53.286\langle P_2\rangle^8\,.\end{aligned} \tag{15}$$

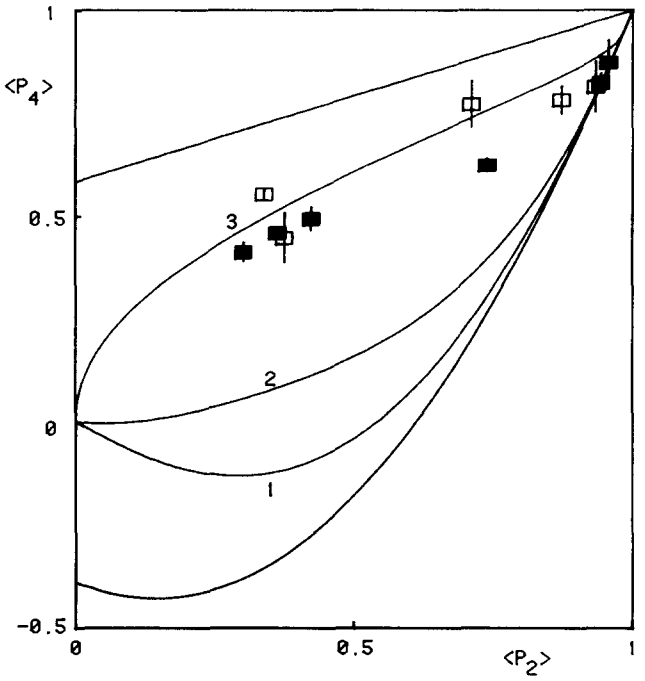

Fig. 7. The experimentally obtained ($\langle P_2\rangle$, $\langle P_4\rangle$) values for DPH in DMPC (⧺) and DPPC (■) at various temperatures are indicated with errorbars on the ($\langle P_2\rangle$, $\langle P_4\rangle$) plane. The *solid lines* represent three existing models relating the $\langle P_2\rangle$ and $\langle P_4\rangle$ values: (1) the cone model; (2) the Gaussian model and (3) the $\langle P_4\rangle$-model. The other two curves are the limitations of the ($\langle P_2\rangle$, $\langle P_4\rangle$)-plane (Kooyman et al. 1983)

Table 3. Reanalysis of the data of DPH in DMPC and DPPC vesicles assuming a priori the $\langle P_4\rangle$-distribution

Lipid	Temperature [°C]	$\langle P_2\rangle$	$\langle P_4\rangle$	D [1/ns]	χ_r^2
DMPC	13.0	0.866 (0.027)	0.833 (0.014)	0.036 (0.006)	3.68
DMPC	14.2′	0.932 (0.007)	0.875 (0.006)	0.061 (0.034)	3.40
DMPC	24.2′	0.707 (0.024)	0.736 (0.016)	0.29 (0.07)	7.22
DMPC	34.1′	0.368 (0.018)	0.517 (0.014)	0.37 (0.02)	2.04
DMPC	34.2	0.335 (0.008)	0.490 (0.006)	0.332 (0.008)	0.84
DPPC	25.6	0.942 (0.003)	0.886 (0.004)	0.043 (0.015)	0.92
DPPC	38.6	0.733 (0.002)	0.753 (0.001)	0.89 (0.02)	1.22
DPPC	45.5′	0.419 (0.006)	0.557 (0.004)	0.73 (0.02)	0.64
DPPC	47.8	0.368 (0.004)	0.516 (0.003)	0.71 (0.01)	0.83
DPPC	55.6′	0.313 (0.007)	0.473 (0.005)	0.78 (0.04)	1.77

The results are given in Table 3. Because $\langle P_2\rangle$ is completely determined by the limiting anisotropy $r(\infty)$ ($r(0)=0.380$ is held fixed in the fitting procedure), it is a model-independent parameter and therefore the values of $\langle P_2\rangle$ in Tables 2 and 3 will nearly be the same. The $\langle P_4\rangle$ value, however, is now calculated from $\langle P_2\rangle$ (Eq. (15)) and is no longer a free parameter in the fit. The only free parameters are now $\langle P_2\rangle$ and D.

From the reduced χ^2-values it is clear that the $\langle P_4\rangle$-distribution may be a possible distribution function for DPH in DMPC and DPPC. The Table confirms the results of Pottel et al. (1986) where a reanalysis of the data of Ameloot et al. (1984) pointed out that the $\langle P_4\rangle$-distribution was indeed a good model for DPH in lipid bilayers.

Remarks

1. With the measured absolute phase angles $\Phi_\parallel$ and $\Phi_\perp$, the absolute modulation amplitudes $m_\parallel$ and $m_\perp$ and the steady-state anisotropy r_s, it is possible to calculate the phase angle difference $\Delta=\Phi_\perp-\Phi_\parallel$ or the differential tangent $\tan\Delta$ and the unnormalized modulation ratio $M=(1+2r_s)\,m_\parallel/[(1-r_s)\,m_\perp]$. These calculated data can be analysed according to the differential method. However, analysis of these data resulted in most cases in very poor fits for $\tan\Delta$ and M due to large scattering in the calculated data. The best result we obtained in this way was for DPH in DMPC at 34.2° and is shown in Fig. 8 a – b.

This result is obtained from the non-linear least squares procedure which minimizes the χ^2-value, here defined as:

$$\chi^2=\sum_\omega \frac{1}{\sigma_\Delta^2}(\tan\Delta_c-\tan\Delta_m)^2+\sum_\omega \frac{1}{\sigma_M^2}(M_c-M_m)^2, \tag{16}$$

where the calculated $\tan\Delta$ and M for the mono-exponential anisotropy decay are given in the appendix. The standard deviations were taken to be $\sigma_\Delta=0.0035$ and $\sigma_M=0.020$. In all other cases, and especially at low temperatures, the results obtained were suspect (large χ_r^2 values and errors). As can be seen from Figs. 3–6, however, the constructed S_D^* and G_D^* data from the same $\Phi_\parallel$, $\Phi_\perp$, $m_\parallel$, $m_\perp$ and r_s show a very small scatter pattern and lead to reasonably well defined anisotropy decay parameters. This is a topic that still needs more investigation.

2. Another remarkable fact we would like to mention here is that the calculated Δ from $\Phi_\parallel$ and $\Phi_\perp$ were not always positive. In fact, the phase angle of the perpendicular component is expected to be larger than that of the parallel component since the fluorophore must rotate into the perpendicular plane of observation in order to be observed through the perpendicular polarizer (Lakowicz et al. 1979).

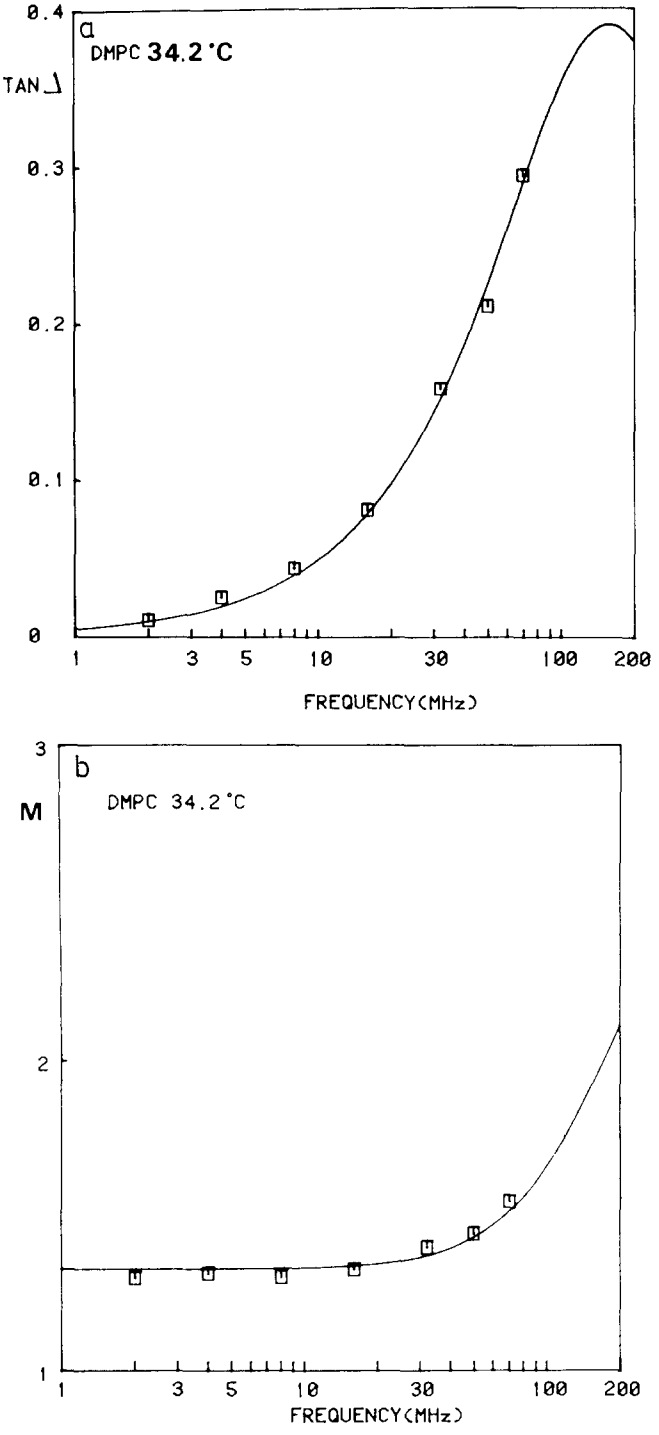

Fig. 8 a and b. The best fit for the hindered rotator model of the $\tan\Delta$ and M values (□) calculated from the measured $\Phi_\parallel$, $\Phi_\perp$, $m_\parallel$, $m_\perp$ and r_s for DPH in DMPC at 34.2 °C is shown as a function of frequency ($r_\infty = 0.061$, $R = 0.88\ \text{ns}^{-1}$, $\chi_r^2 = 2.99$)

From the measured absolute phase angles $\Phi_\parallel$ and $\Phi_\perp$, Δ was sometimes found to be negative, that is $\Phi_\parallel > \Phi_\perp$. The calculated differential tangent was then negative and not useful while the calculated S_D^* and G_D^* from the same phase angles and modulation ratios could still be used as valuable data. Zavoico et al. (1985) and Gratton et al. (private communication) even found negative $\tan\Delta$, when Δ or $\tan\Delta$ was measured directly by the method of Weber (1977). However, it must be noted that in all our cases, the negative phase angle differences were at low frequencies and/or at low temperatures (below T_{tr}).

Table 4. Anisotropy decay parameters for DPH in DMPC vesicles obtained from $\tan\Delta$ and M (hindered rotator model)

Temperature [°C]	τ [ns]	r_s	R [ns^{-1}]	r_∞	χ_r^2
14.2	10.9	0.3368	0.45 (0.06)	0.325 (0.003)	1.66
24.2	10.1	0.2200	0.57 (0.03)	0.187 (0.003)	1.77
34.1	8.8	0.0967	0.69 (0.02)	0.051 (0.003)	1.01

3. With the SLM 4800A Subnanosecond Spectrofluorometer, the differential tangent was also measured directly by the method of Weber (1977) for DPH in DMPC. The modulation ratio M was again calculated from $m_\parallel$, $m_\perp$ and r_s. A remarkable fact is that when Δ or $\tan\Delta$ was measured directly only positive values were obtained, while the calculated Δ from the measured absolute phase angles $\Phi_\parallel$ and $\Phi_\perp$ for DMPC at 14.2° at 6 and 30 MHz were found to be negative.

The anisotropy decay parameters R and r_∞ for DPH in DMPC at the temperatures 14.2°, 24.2° and 34.1° are given in Table 4.

Note that the χ_r^2-value and the parameter errors are smaller than those obtained from the transform method (Table 2). However, in all of these three cases, and most pronounced at low temperatures, the deviations between the calculated $\tan\Delta$ and M and the measured quantities were larger than those between the calculated and measured S_D^* and G_D^* (see Figs. 9 a – b).

This lower χ_r^2 can only be due to the choice of the estimated standard deviations σ_Δ and σ_M from which the weights in the χ^2 value were calculated. This difference in χ_r^2, favourable to the differential method is also not expected from the theoretical point of view as explained in the previous paper. Theoretically one should expect the transform method to be better at low temperatures because r_s and r_∞ are large. As an example, the data and results for DMPC 14.2° are shown in Fig. 10 a – b. In Fig. 5, the sine and cosine transform are plotted for the same system and temperature. From these figures it can be seen that nearly the whole S_D^* and G_D^* patterns are obtained within the region of

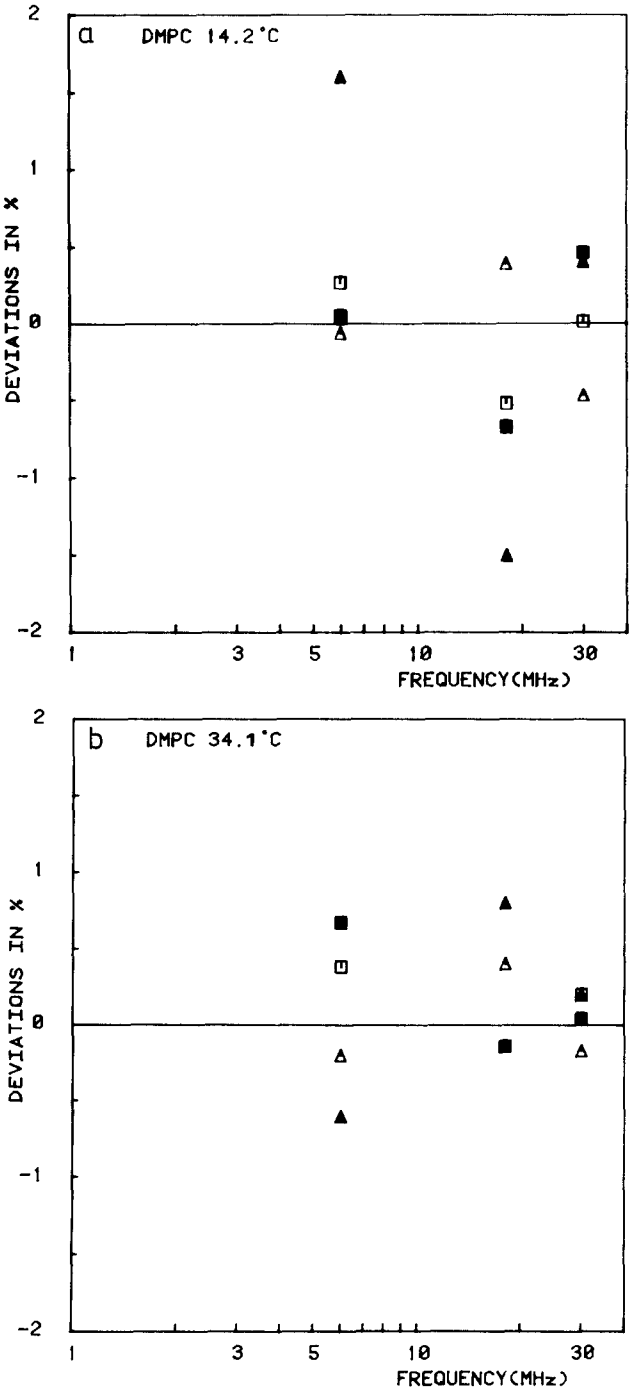

Fig. 9 a and b. The percentage deviations between the calculated and the measured quantities for $\tan\Delta$ (■), M (▲) were compared to the deviations of G_D^* (△) and S_D^* (□) for DPH in DMPC below (14.2 °C) and above (34.1 °C) the phase transition. The $\tan\Delta$, M, S_D^* and G_D^* were calculated from the hindered rotator model

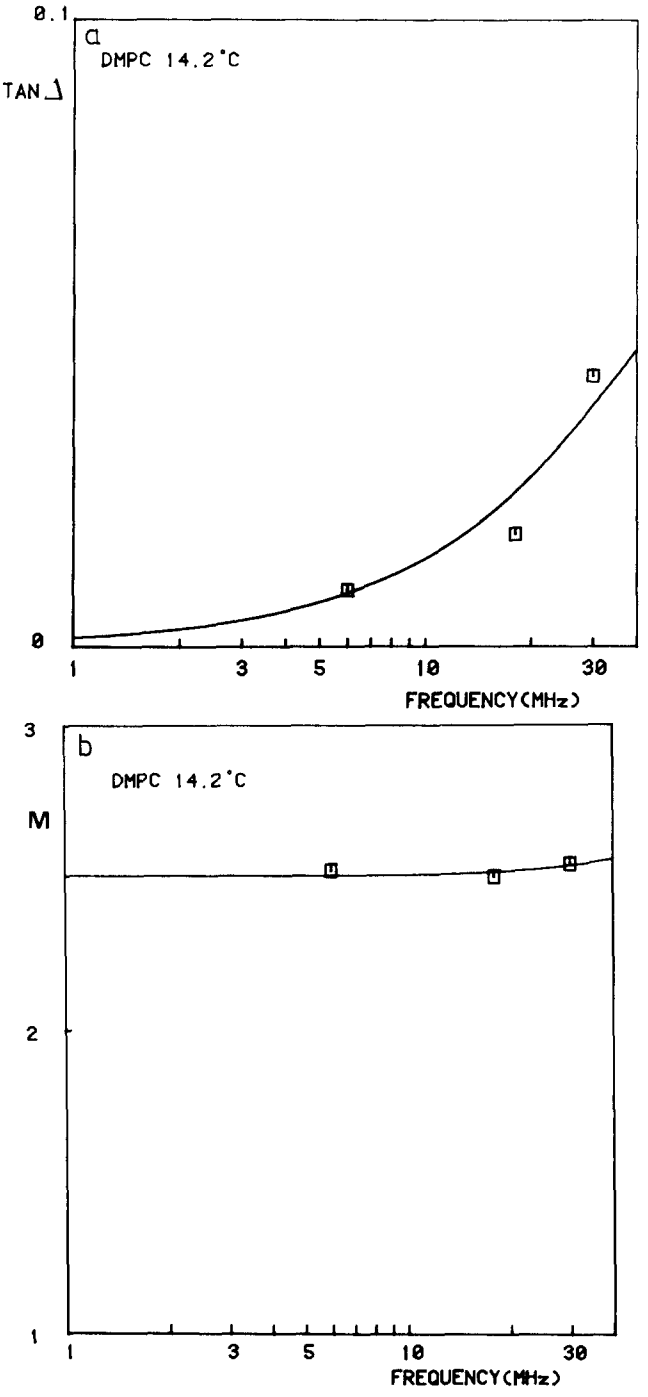

Fig. 10 a and b. The differential tangent $\tan\Delta$ and the modulation ratio M obtained directly from the differential method at three frequencies 6, 18 and 30 MHz are shown (□). The best fit calculated from the hindered rotator model is also indicated (*solid curves*) as a function of frequency

30 MHz, while the maximum of the differential tangent is not even reached and the modulation ratio has hardly changed in this frequency interval.

4. An attempt has been made to fit the differential tangent and the modulation ratio, calculated from the general model to the DMPC data obtained with the differential method. Although $\langle P_2 \rangle$ was a relatively stable parameter in the fit, several ($\langle P_4 \rangle$, D) sets were obtained, depending on the starting values in the computer program and resulting in practically the same χ_r^2. This result must be

Table 5. Anisotropy decay parameters for DPH in DMPC vesicles obtained from tan Δ and M (general model)

Temperature [°C]	τ [ns]	r_s	$\langle P_2 \rangle$	$\langle P_4 \rangle$	D [ns^{-1}]	χ_r^2
14.2	10.9	0.3368	0.926 (0.005)	0.788 (0.089)	0.011 (0.002)	1.81
24.2	10.1	0.2200	0.683 (0.012)	0.744 (0.152)	0.32 (0.52)	5.09
34.1	8.8	0.0967	0.305 (0.034)	0.523 (0.108)	0.34 (0.24)	1.95

due to the fact that both the differential tangent and the modulation ratio are insensitive to the influence of $\langle P_4 \rangle$ in the restricted frequency region of 30 MHz. In Table 5, the best result for the general model fit is given. In spite of the fact that unreasonably small errors were always obtained with the differential method (Lakowicz et al. 1985), the parameter errors in Table 5 are larger than those obtained with the transform method (see Table 4).

5. We note that the recent commercial availability of true multifrequency phase fluorometers (I.S.S., Inc.) will diminish the use of the classic 6, 18, 30 MHz instruments. However, the large number of these three frequencies machines in laboratories around the world will assure their use for some time and justifies the analysis presented here.

Conclusion

The data presented above clearly illustrate the value of our new alternative analysis procedure when applied to anisotropic lipid systems.

We do not pretend that the same information about the dynamics of a fluorophore in such a system can not be obtained from the measurement of the phase-angle difference and the modulation ratio. However, our results were obtained by changing the frequency over a rather restricted frequency region ([0, 30 MHz], [0, 70 MHz] or [0, 100 MHz]) where we used only 3, 7 or 8 frequencies respectively. This can be done because the sine and cosine transforms S_D^* and G_D^* are spread out over a much smaller frequency region than the differential tangent and the modulation ratio. Our results suggest that the transform method is the most sensitive one in the frequency region [0, 30 MHz].

Nevertheless, lower reduced χ^2 values were found when the differential data was fitted. Also, very small errors in the parameters were found. Lakowicz et al. (1985) also mentioned the unreasonably small errors in the parameters as a topic which requires more investigation.

Acknowledgements. The work reported here started when one of us (BWV) was visiting the laboratories of Dr. Michael Glaser and Dr. Enrico Gratton at the University of Illinois at Urbana-Champaign. We thank them for their support and hospitality. Thanks are also due to Dr. Enrico Gratton for the use of his instrument and helpful discussions. The technical assistance of Earl Martin (Urbana, IL) in preparing lipid vesicles is gratefully acknowledged. We also thank Dr. David Jameson (Dallas, TX) for his stimulating suggestions and comments and Dr. Marcel Ameloot (Diepenbeek, Belgium) for his help with the computer programs.

Appendix

1. Mono-exponential anisotropy decay:

$$r(t) = (r_0 - r_\infty) \exp(-R\,t) + r_\infty .$$

The sine and cosine transforms S_D^* and G_D^* and the steady-state anisotropy r_s, calculated from Eqs. (5a–c) and using the mono-exponential fluorescence decay function

$$I(t) = 1/\tau \exp(-t/\tau)$$

are

$$S_D^* = \omega\,\tau \left[\frac{r_\infty}{1+\omega^2\tau^2} + \frac{r_0 - r_\infty}{(1+R\,\tau)^2 + \omega^2\tau^2} \right] \tag{A1}$$

$$G_D^* = \frac{r_\infty}{1+\omega^2\tau^2} + (r_0 - r_\infty)\frac{1+R\,\tau}{(1+R\,\tau)^2+\omega^2\tau^2} \tag{A2}$$

$$r_s = r_\infty + \frac{r_0 - r_\infty}{1+R\,\tau}, \tag{A3}$$

where $\omega = 2\pi f$ and f is the modulation frequency in MHz. The expressions for the differential tangent $\tan\Delta$ and the unnormalized modulation ratio M are:

$$\tan\Delta = \frac{3\,\omega\,\tau\,(r_0 - r_\infty)\,R\,\tau}{m_0\,(1+\omega^2\tau^2) + S\,R\tau + m_\infty\,(R\,\tau)^2} \tag{A4}$$

$$M = \left[\frac{\omega^2\tau^2\,(1+2\,r_0)^2\,(r_s - r_\infty)^2 + (r_0 - r_\infty)^2\,(1+2\,r_s)^2}{\omega^2\tau^2\,(1-r_0)^2\,(r_s - r_\infty)^2 + (r_0 - r_\infty)^2\,(1-r_s)^2} \right]^{1/2}, \tag{A5}$$

where $m_0 = (1+2\,r_0)(1-r_0)$, $m_\infty = (1+2\,r_\infty)(1-r_\infty)$ and $S = 2 + r_0 - r_\infty(4\,r_0 - 1)$.

2. General model:

$$r(t) = r_0[\beta_0 \exp(-\alpha_0 t) + 2\,\beta_1 \exp(-\alpha_1 t) + 2\,\beta_2 \exp(-\alpha_2 t)] + r_0\langle P_2\rangle^2 .$$

The pre-exponential and exponential factors are:

$$\begin{aligned}
\beta_0 &= 1/5 + 2/7\langle P_2\rangle + 18/35\langle P_4\rangle - \langle P_2\rangle^2 \\
\beta_1 &= 1/5 + 1/7\langle P_2\rangle - 12/35\langle P_4\rangle \\
\beta_2 &= 1/5 - 2/7\langle P_2\rangle + 3/35\langle P_4\rangle \\
\alpha_0 &= 6\,D_\perp(1/5 + 1/7\langle P_2\rangle - 12/35\langle P_4\rangle)/\beta_0 \\
\alpha_1 &= 6\,D_\perp(1/5 + 1/14\langle P_2\rangle + 8/35\langle P_4\rangle)/\beta_1 \\
\alpha_2 &= 6\,D_\perp(1/5 - 1/7\langle P_2\rangle - 2/35\langle P_4\rangle)/\beta_2 .
\end{aligned} \tag{A6}$$

The calculated S_D^*, G_D^* and r_s are then:

$$S_D^* = \omega\tau\left[\frac{r_0\langle P_2\rangle^2}{1+\omega^2\tau^2} + \frac{r_0\beta_0}{(1+\alpha_0\tau)^2+\omega^2\tau^2}\right. \quad \text{(A7)}$$
$$\left. + \frac{2r_0\beta_1}{(1+\alpha_1\tau)^2+\omega^2\tau^2} + \frac{2r_0\beta_2}{(1+\alpha_2\tau)^2+\omega^2\tau^2}\right].$$

$$G_D^* = \frac{r_0\langle P_2\rangle^2}{1+\omega^2\tau^2} + \frac{r_0\beta_0(1+\alpha_0\tau)}{(1+\alpha_0\tau)^2+\omega^2\tau^2} \quad \text{(A8)}$$
$$+ \frac{2r_0\beta_1(1+\alpha_1\tau)}{(1+\alpha_1\tau)^2+\omega^2\tau^2} + \frac{2r_0\beta_2(1+\alpha_2\tau)}{(1+\alpha_2\tau)^2+\omega^2\tau^2}.$$

$$r_s = r_0\langle P_2\rangle^2 + \frac{r_0\beta_0}{1+\alpha_0\tau} + \frac{2r_0\beta_1}{1+\alpha_1\tau} + \frac{2r_0\beta_2}{1+\alpha_2\tau}. \quad \text{(A9)}$$

The expressions for $\tan\Delta$ and $m_\parallel/m_\perp$ can be found in the paper of Van der Meer et al. (1984).

References

Ameloot M, Hendrickx H, Herreman W, Pottel H, Van Cauwelaert F, Van der Meer BW (1984) Effect of orientational order on the decay of the fluorescence anisotropy in membrane suspensions: Experimental verification on unilamellar vesicles and lipid/α-lactalbumin complexes. Biophys J 46: 525–539

Barrow DA, Lentz BR (1985) Membrane structural domains. Resolution limits using diphenylhexatriene fluorescence decay. Biophys J 48: 221–234

Bevington PR (1969) Data reduction and error analysis for the physical science. McGraw-Hill, New York

Chen LA, Dale RE, Roth S, Brand L (1977) Nanosecond time-dependent fluorescence depolarization of diphenylhexatriene in dimyristoyllecithin vesicles and the determination of "microviscosity". J Biol Chem 252: 2163–2169

Chong PL, Van der Meer BW, Thompson TE (1985) The effects of pressure and cholesterol on rotational motions of perylene in lipid bilayers. Biochim Biophys Acta 813: 253–265

Dale RE, Chen LA, Brand L (1977) Rotational relaxation of the "microviscosity" probe diphenylhexatriene in paraffin oil and egg lecithin vesicles. J Biol Chem 252: 7500–7510

Depauw H, De Wolf M, Van Dessel G, Hilderson HJ, Lagrou A, Dierick W (1985) Fluidity characteristics of bovine thyroid plasma membranes. Biochim Biophys Acta 814: 57–67

Gratton E, Limkeman M (1983) A continuously variable frequency cross-correlation phase fluorometer with picosecond resolution. Biophys J 44: 315–324

Johnson LW, Zilversmit DB (1975) Catalytic properties of phospholipid exchange protein from bovine heart. Biochim Biophys Acta 375: 165–175

Kinosita K Jr, Kawato S, Ikegami A (1977) A theory of fluorescence depolarization decay in membranes. Biophys J 20: 289–305

Klausner RD, Kleinfeld AM, Hoover RL, Karnovsky MJ (1980) Lipid domain in membranes: evidence derived from structural perturbations induced by free fatty acids and lifetime heterogeneity analysis. J Biol Chem 255: 1286–1295

Koymann RPH, Levine YK, van der Meer BW (1981) Measurement of second and fourth rank order parameters by fluorescence polarization experiments in a lipid membrane system. Chem Phys 60: 317–326

Lakowicz JR, Prendergast FG (1978a) Detection of hindered rotations of 1,6-diphenyl-1,3,5-hexatriene in lipid bilayers by differential polarized phase fluorometry. Biophys J 24: 213–231

Lakowicz JR, Prendergast FG (1978b) Quantitation of hindered rotations of diphenylhexatriene in lipid bilayers by differential polarized phase fluorometry. Science 200: 1399–1401

Lakowicz JR, Prendergast FG, Hogen D (1979) Differential polarized phase fluorometric investigations of diphenylhexatriene in lipid bilayers. Quantitation of hindered depolarizing rotations. Biochemistry 18: 508–519

Lakowicz JR, Gratton E, Cherek H, Maliwal BP, Lackzo G (1984a) Determination of time-resolved fluorescence emission spectra and anisotropies of a fluorophore-protein complex using frequency domain phase-modulation fluorometry. J Biol Chem 259: 10967–10972

Lakowicz JR, Lackzo G, Cherek H, Gratton G, Limkeman M (1984b) Analysis of fluorescence decay kinetics from variable frequency phase shift and modulation data. Biophys J 46: 463–477

Lakowicz JR, Cherek H, Maliwal BP, Gratton E (1985) Time-resolved fluorescence anisotropies of diphenylhexatriene and perylene in solvents and lipid bilayers obtained from multifrequency phase-modulation fluorometry. Biochemistry 24: 376–383

Lentz B, Barenholz Y, Thompson TE (1976) Fluorescence depolarization studies of phase transitions and fluidity in phospholipid bilayers. 2. Two-component phosphatidylcholine liposomes. Biochemistry 15: 4529–4536

Mantulin WW, Weber G (1977) Rotational anisotropy and solvents fluorophore bonds: An investigation by differential polarized phase fluorometry. J Chem Phys 66: 4092–4099

Pottel H, Herreman W, Van der Meer BW, Ameloot M (1986) On the significance of the fourth rank orientational order parameter of fluorophores in membranes. Chem Phys 102: 37–44

Spencer RD, Weber G (1969) Measurements of subnanosecond fluorescence lifetimes with a cross-correlation phase fluorometer. Ann NY Acad Sci 158: 361–376

Spencer RD, Weber G (1970) Influence of Brownian rotations and energy transfer upon the measurements of fluorescence lifetime. J Chem Phys 52: 1654–1663

Stubbs CD, Kouyama T, Kinosita K Jr, Ikegami A (1981) Effect of double bonds on the dynamic properties of the hydrocarbon region of lecithin bilayers. Biochemistry 20: 4257–4262

Szabo A (1984) Theory of fluorescence depolarization in macromolecules and membranes. J Chem Phys 81: 150–167

Van der Meer BW, Pottel H, Herreman W, Ameloot M, Hendrickx H, Schröder H (1984) Effect of orientational order on the decay of the fluorescence anisotropy in membrane suspensions: A new approximate solution of the rotational diffusion equation. Biophys J 46: 515–523

Van der Meer BW, Pottel H, Herreman W (1987) A new approach to polarized fluorescence using phase and modulation fluorometry. I. Theory with reference to hindered and anisotropic rotations. Eur Biophys J 15: 35–45

Weber G (1977) Theory of differential phase fluorometry. Detection of anisotropic molecular rotations. J Chem Phys 66: 4081–4091

Weber G (1978) Limited rotational motion: Recognition by differential phase fluorometry. Acta Phys Pol A54: 859–865

Zannoni C (1979) Mean field theory of a model anisotropic potential of rank higher than two. Mol Cryst Liq Cryst 49 (Letters): 247–253

Zavoico GB, Chandler L, Kutchai H (1985) Perturbation of egg phosphatidylcholine and dipalmitoylphosphatidylcholine multilamellar vesicles by n-alkanols. A fluorescent probe study. Biochim Biophys Acta 812: 219–312